

# V-band Integrated Filter and Antenna for LTCC Front-End modules

Jong-Hoon Lee<sup>(1)</sup>, Nobutaka Kidera<sup>(2)</sup>, Stephane Pinel<sup>(1)</sup>, Joy Laskar<sup>(1)</sup> and Manos M. Tentzeris<sup>(1)</sup>

<sup>(1)</sup>Georgia Electronic Design Center, School of Electrical and Computer Engineering  
Georgia Institute of Technology, Atlanta, GA 30332-0269, USA..

<sup>(2)</sup>Asahi Glass Co., Ltd. 1150 Hazawa-cho, Kanagawa-ku, Yokohama, Kanagawa 221-8755, Japan  
Fax: (404)894-0222, Email: jonglee@ece.gatech.edu

**Abstract** – In this paper, fully integrated filter and antenna functions are demonstrated as a system-on-package (SOP) compact front-end solution for the low-temperature cofired ceramic (LTCC) based V-band modules. The compact and easy-to-design integrated passive functions of filter and antenna have been hereby experimentally validated. A 4-pole quasi-elliptic band pass filter composed of four open loop resonators has been developed. It exhibits an insertion loss < 3.48 dB, a return loss > 15 dB over the pass band (~3.4 GHz) and a 3dB bandwidth of about 5.46 % (~3.4 GHz) at the center frequency of 62.3 GHz. In addition, a series fed 1by4 linear array antenna of four microstrip patches exhibiting high gain and fan-beam radiation pattern has been designed in a way that allows for an easy integration into a V-band multi-gigabit-per-second wireless link system. Its 10 dB bandwidth is experimentally validated to be 55.4-66.8 GHz (~18.5 %). The above proposed designs have been combined together, leading to the complete passive integration with high level of selectivity over the band of interest. The excellent overall performance of the integrated solution is verified through a 10 dB bandwidth of 4.8 GHz (59.2 – 64 GHz) and a return loss > 10.47 dB over the passband.

**Index Terms** –quasi-elliptic filters, open loop resonator, low-temperature co-fired ceramic (LTCC), patch antenna, system-on-package (SOP), V-band, front-end module, integrated passives, mm-wave.

## I. INTRODUCTION

The dramatic increase of interest in license-free spectrum around 60 GHz is led by the high-data rate applications such as high-speed internet access, video streaming, content downloads, and wireless data bus for cable replacement [1]. Such emerging applications with data rate greater than 2 Gb/s require real estate efficiency, low-cost manufacturing, and excellent performance achieved by a high level of integration of embedded functions using low-cost and high-performance materials such as the multilayer low-temperature cofired ceramic (LTCC) [2]. The optimal integration of RF passives into 60 GHz (V-band) front-end module is significantly challenging since the electrical performance can be degraded by severe parasitic and interconnection losses. The microwave structures for integrating filter and antenna function which is commonly called a filtering antenna have been implemented using stacked cavities coupled by a metallic iris at K-band [3], an

electromagnetic horn [4] and a leaky waveguide [5] at X-band. Despite of their large size, these topologies show that the integrated filter and antenna functions have a great potential to be integrated into higher frequencies modules.

In this paper, we present compact and high-performance passive building blocks and their integration, enabling a complete passive integration solution for 3D compact, low-cost wireless V-band front-end modules. The section II of this paper discusses the development of a 4-pole cross-coupled quasi-elliptic filter, targeting high selectivity and compactness. Section III concentrates on the design of a series fed 1×4 linear array antenna of four micro-strip patches covering 59-64 GHz. This high-gain and directive antenna is suited for point-to-point applications in short-range indoor wireless personal area network (WPAN) and can be easily integrated into a V-band module. The complete integration of the above developed filter and antenna was successfully implemented with a planar transition as described in section IV. The integrated front-end demonstrates the excellent band selectivity through a 10-dB bandwidth of approximately 4.8 GHz (59.2 – 64 GHz) and return loss >10.47 dB over the passband.

## II. 4-POLE QUASI-ELLIPTIC FILTER

As the demand for highly selective, compact and low loss band pass filters increases in multi-gigabit-per-second wireless communication systems, the coupled open-loop resonator filter becomes a candidate of choice for the integration of V-band front-end modules. Numerous researchers [6-8] have demonstrated narrow bandwidth filters employing open-loop resonators for current mobile communication services at L and S bands. In this section, the design of a 4-pole quasi-elliptic filter is presented as a filter solution for LTCC 60 GHz front-end module. This filter is chosen because it provides only one pair of transmission zeros at finite frequencies to satisfy the desired specifications (listed below), exhibiting much improved skirt selectivity and making it a feasible intermediate between the Chebyshev and elliptical-function filters [7]. At millimeter-wave frequencies, the design of the coupled open-loop resonator filter is very challenging because of the design rules limitations of the process. Nevertheless, the

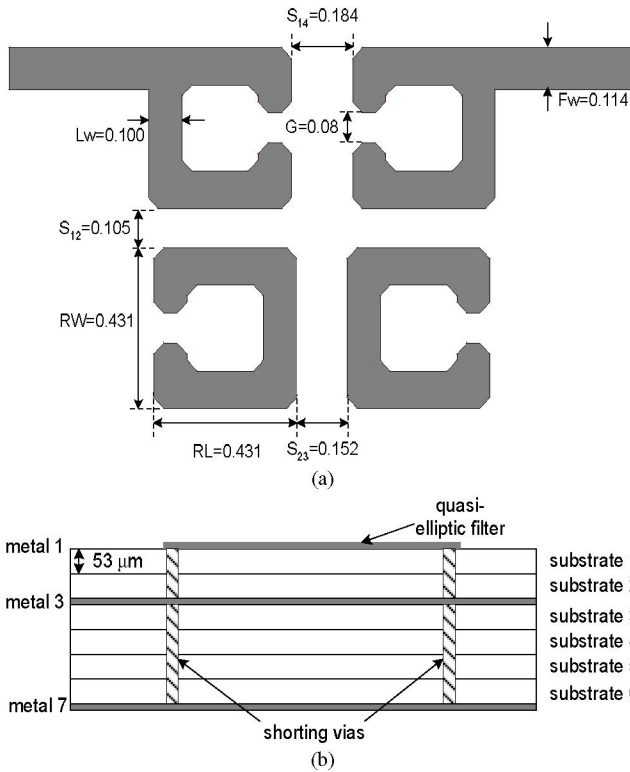


Figure 1. (a) Top view and (b) cross-section view of 4-pole quasi-elliptic band pass filter consisting of open-loop resonators fabricated on LTCC. All dimensions indicated in (a) are in mm.

very mature multilayer fabrication capabilities of LTCC ( $\epsilon_r=7.1$ ,  $\tan\delta=0.0019$ , metal layer thickness:  $9\ \mu\text{m}$ , number of layers: 6, dielectric layer thickness:  $53\ \mu\text{m}$ , minimum metal line width and spacing: up to  $75\ \mu\text{m}$ ) appear to be a competitive solution to meet millimeter-wave design requirements in terms of physical dimension of the open-loop resonators ( $\approx 0.2\lambda_g \times 0.2\lambda_g$ ) and spacing ( $\geq 80\ \mu\text{m}$ ) between adjacent resonators that determine the coupling coefficient of the filter function.

All designs have been simulated using the MOM-based, 2.5 full-wave solver IE3D. Fig. 1 (a), (b) shows the top view and cross-section view of the quasi-elliptic band pass filter, respectively. The filter was designed according to the filter synthesis proposed by Hong [7] to meet the following specifications: (1) center frequency: 62 GHz (2) fractional bandwidth: 5.61% ( $\sim 3.5\text{GHz}$ ) (3) insertion loss:  $< 3\text{dB}$  (4) 35 dB rejection bandwidth: 7.4 GHz. The effective length (RL in Fig 1 (a)) and width (RW in Fig 1 (a)) of the open resonator has been chosen to be equal to  $0.2\lambda_g$ . The design parameters such as the coupling coefficients ( $C_{12}$ ,  $C_{23}$ ,  $C_{34}$ ,  $C_{14}$ ) and the external quality factor ( $Q_{\text{ext}}$ ) can be theoretically calculated based on the element values of a 4-pole low-pass prototype [7]. The calculated design parameters are:

$$C_{12}=C_{34}=0.048, C_{14}=-0.012 \\ C_{23}=0.044, Q_{\text{ext}}=17.001.$$

To determine the physical spacing between resonators, full-wave simulations (IE3D) were used to extract the coupling coefficients and external quality factors [7]. The

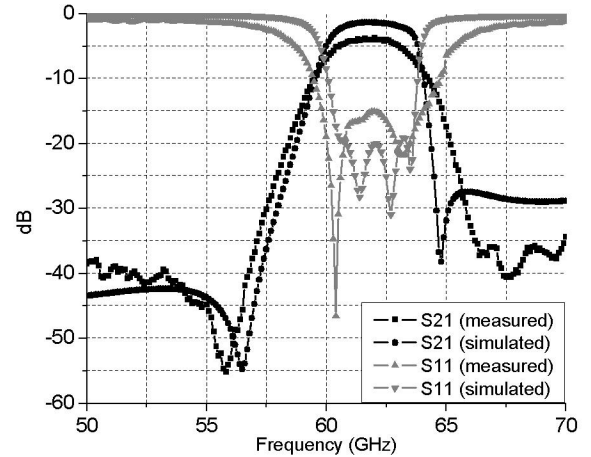


Figure 2. The comparison between measured and simulated S-parameters ( $S_{21}$  &  $S_{11}$ ) of the 4-pole quasi-elliptic band pass filter composed of open-loop resonators.

quasi elliptic filter was fabricated on the first metallization layer (metal 1 in Fig 1. (b)), which is placed two substrate layers ( $\sim 106\ \mu\text{m}$ ) above the first ground plane on metal 3. This ground plane is connected to the second ground plane located on the back side of the substrate through shoring vias (pitch:  $390\ \mu\text{m}$ , diameter:  $130\ \mu\text{m}$ ) as shown in Fig. 1 (b). The fabricated filter occupies  $3.075 \times 1.455 \times 0.106\ \text{mm}^3$  ( $\sim 1.40\lambda_g \times 0.66\lambda_g \times 0.048\lambda_g$ ) including feeding structures and CPW measurement pads.

Fig. 2 shows the comparison between the simulated and measured S parameters of the band pass filter. The filter exhibits an insertion loss  $< 3.48\ \text{dB}$  which is higher than the simulated values of  $< 1.37\ \text{dB}$  and a return loss  $> 15\ \text{dB}$  compared to a simulated value of  $< 21.9\ \text{dB}$  over the passband. The loss discrepancy can be attributed to conductor loss caused by skin and edge effect of metal traces since the simulations assume a perfect definition of metal strips. The measurement shows a slightly decreased 3-dB fractional bandwidth of 5.46% ( $\sim 3.4\ \text{GHz}$ ) at a center frequency of 62.3 GHz. The simulated results give a 3 dB bandwidth of 5.61% ( $\sim 3.5\ \text{GHz}$ ) at a center frequency 62.35 GHz. The transmission zeros are observed within  $< 5\ \text{GHz}$  away from the cut-off frequency of the passband. The discrepancy of the zero positions between the measurement and the simulation can be attributed to the fabrication tolerance. However, the overall response of the measurement correlates very well with the simulation.

### III. SERIES FED ARRAY ANTENNA

The growing interest of high-data rate applications such as high-speed Internet access naturally motivates the development of compact antenna array exhibiting the high gain and fan-beam radiation that is wide in azimuth and narrow in elevation. The antenna dimensions are inversely proportional to carrier frequency so that for a fixed physical area, the number of elements in the array can be increased to compensate for the high path loss at 60 GHz.

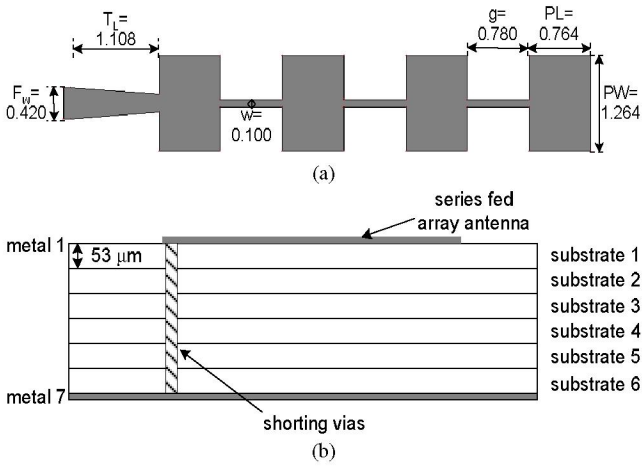
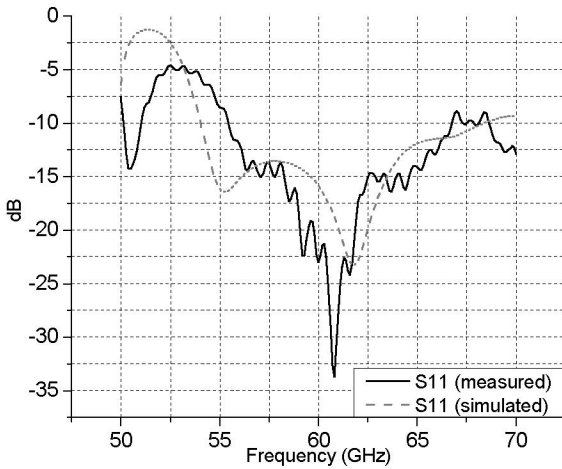
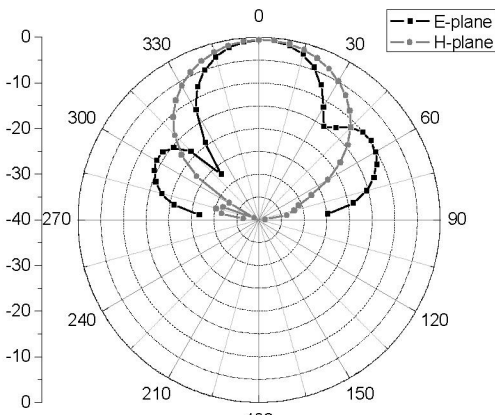


Figure 3. (a) Top view and (b) cross-section view of a series fed  $1 \times 4$  linear array of four microstrip patches. All dimensions indicated in (a) are in mm.



(a)



(b)

Figure 4. (a) The comparison between measured and simulated return loss (S11) (b) radiation characteristics at 61.5 GHz of a series fed  $1 \times 4$  array antenna

In this section, a series fed  $1 \times 4$  linear array antenna of four microstrip patches [9] covering 59–64 GHz has been

designed on LTCC substrate and its top view and cross-section view are illustrated in Fig. 3 (a) and (b), accordingly. The proposed antenna employs a series feed instead of a corporate feed [9] because of its easy-to-design feeding network without any requirements of power splitters. The matching between neighbouring elements is performed by controlling the width (PW in Fig. 3 (a)) of the patch elements. The antenna was screen-printed on the top metal layer (metal 1 in Fig. 3 (b)), and uses six substrate layers to provide the required broadband matching property and high gain. The targeted operation frequency was 61.5 GHz. First, the single patch resonator ( $0.378\lambda_g \times 0.627\lambda_g$ ) resonating at 61.5 GHz is designed. Then, identical four patch resonators are linearly cascaded using thin microstrip lines ( $w=0.100$ mm in Fig. 3(a)). The distance ( $g$  in Fig. 3 (a)) between patch elements is the critical design parameter to achieve equal amplitude and co-phase excitation and control the tilt of the maximum beam direction. It was optimized to be 0.780 mm ( $\sim 0.387\lambda_g$ ) for  $0^\circ$  tilted fan beam antenna. A Klopfenstein tapered microstrip transition [10] was utilized between the patch and the  $50\Omega$  feeding line. Its length was determined to be 1.108 mm ( $T_L$  in Fig. 3 (a)). Fig. 4 (a) shows very good correlation between the measured and simulated return loss (S11) versus frequency for the design. The measured 10-dB bandwidth is 55.4–66.8 GHz ( $\sim 18.5\%$ ) compared to the simulated which is 54–68.4 GHz ( $\sim 23.4\%$ ). The narrower bandwidth might be due to the band limiting effect from the measurement pad. Fig. 4 (b) presents E-plane and H-plane radiation patterns at the center frequency of 61.5 GHz. We can easily observe the  $0^\circ$  beam tilt from the radiation characteristics. The maximum gain of this antenna is 12.6 dBi.

#### IV. INTEGRATION

In 60 GHz front-end module development, the compact integration of the antenna and filter is a crucial issue in terms of real estate efficiency and performance improvement such as high level of band selectivity, spurious suppression and low filtering loss.

Using the developed quasi-elliptic filter and the series-fed array antenna, it is now possible to realize a V-band compact integrated front-end. The 3D overview and cross-section view of the topology chosen for the integration are shown in Fig. 5 (a) and (b) respectively. The 4-pole quasi-elliptic filter and the  $1 \times 4$  series fed array antenna are located on the top metallization layer (metal1 in Fig. 5 (b)) and are connected together with a tapered microstrip transition as shown in Fig 5 (a). The ground planes of the filter and the antenna are located on metal 3, on metal 7, respectively. The ground plane of the filter is terminated at the edge of the antenna feedline, and the two ground planes on metal 3 and 7 are connected together with a via array as presented in Fig. 5. The design of the tapered microstrip transition aims to annihilate the parasitic modes from the  $50\Omega$  microstrip lines discontinuities between the two devices and to maintain a good impedance matching. The

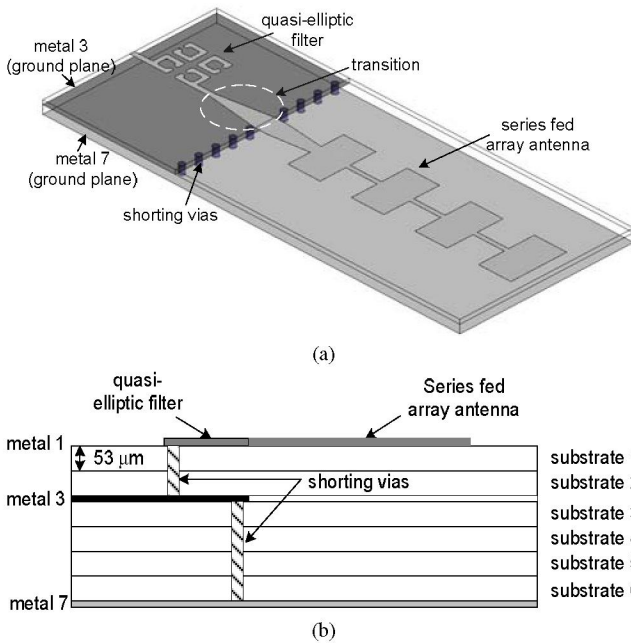


Figure 5. (a) The 3D overview and (b) cross-section view of the integrated filter and antenna functions. All dimensions indicated are in mm.

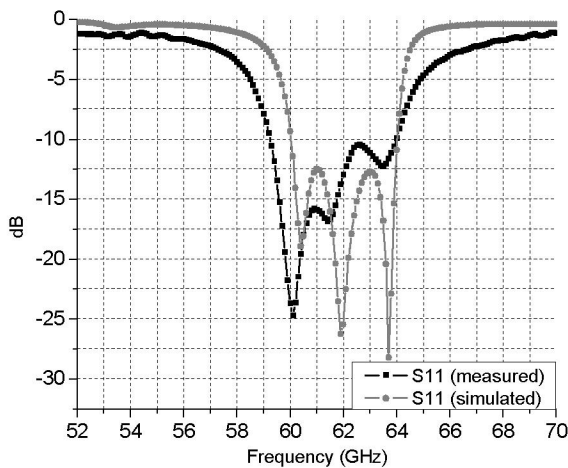


Figure 6. The comparison between measured and simulated return loss (S11) of the integrated filter and antenna functions

fabricated integrated front-end occupies an area of  $9.616 \times 1.542 \times 0.318 \text{ mm}^3$  including CPW measurement pads.

Fig. 6 shows the simulated and measured return losses of the integrated structure. It is observed that the 10-dB return loss bandwidth is approximately 4.8 GHz (59.2 – 64 GHz) that is slightly wider than the simulation of 4 GHz (60–64 GHz). The slightly increased bandwidth may be attributed to the parasitic radiation from the feedlines and from the transition, as well as from the edges effects of the discontinuous ground planes.

## V. CONCLUSION

In this work, fully integrated filter and antenna functions are demonstrated as a system-on-package (SOP) compact front-end solution for the LTCC-based V-band modules. A

front-end prototype demonstrates the excellent performance of compact and easy-to-design passive components and their integration capability. The 4-pole quasi-elliptic filter achieves a high level of band selectivity and a great compromise between size and insertion loss. The filter provides an insertion loss  $< 3.48 \text{ dB}$ , a return loss  $> 15 \text{ dB}$  over the pass band ( $\sim 3.4 \text{ GHz}$ ) and a 3dB bandwidth of about 5.46 % ( $\sim 3.4 \text{ GHz}$ ) at the center frequency of 62.3 GHz. In addition, a series fed  $1 \times 4$  linear array antenna of four microstrip patches exhibiting high gain and fan-beam radiation pattern has been designed for an easy integration into a V-band multi-gigabit-per-second wireless link system. Its 10-dB bandwidth is experimentally validated to be 55.4–66.8 GHz ( $\sim 18.5 \%$ ). The developed filters and antennas have been combined together, leading to a complete passive front-end integration with high level of selectivity over the band of interest. The excellent performance of the integrated solution is verified through a 10 dB return loss bandwidth of 4.8 GHz (59.2 – 64 GHz).

## ACKNOWLEDGEMENT

The authors wish to acknowledge the support of Asahi Glass Co., the Georgia Tech. Packaging Research Center, the Georgia Electronic Design Center, the NSF CAREER Award #ECS-9984761, and the NSF Grant #ECS-0313951.

## REFERENCES

- [1] H.H.Meinel, "Commercial Applications of Millimeterwaves History, Present Status, and Future Trends," *IEEE Transaction on Microwave Theory and Technique*, Vol. 43, NO. 7, pp. 1639-1653, July 1995.
- [2] J.Lee, G.DeJean, S.Sarkar, S.Pinel, K.Lim, J.Papapolymerou, J.Laskar, and M.M.Tentzeris, "Highly Integrated Millimeter-Wave Passive Components Using 3-D LTCC System-on-Package (SOP) Technologies," *IEEE Transaction on Microwave Theory and Technique*, vol.53, pp. 2220-2229, June 2005.
- [3] H.Blondeaux, D.Baillargeat, P.Leveque, S.Verdeyme, P.Vaudon, P.Guillon, A.Carlier, and Y.Cailloce, "Microwave Device combining Filtering and Radiating Functions for Telecommunication Satellites," in *2001 IEEE MTT-S Int. Microwave Sym. Dig.*, Phoenix, AZ, May 2001, pp. 137-140.
- [4] B.Fropplier, Y.Mahe, E.M.Cruz, and S.Toutain, "Integration of a Filtering in an Electromagnetic Horn," in *2003 IEEE European Microwave Symposium*, Munich, Germany, Oct. 2003, pp. 939-942.
- [5] F.Queudet, B.Fropplier, Y.Mahe, and S.Toutain, "Study of a Leaky Waveguide for the Design of Filtering Antennas," in *2003 IEEE European Microwave Symposium*, Munich, Germany, Oct. 2003, pp. 943-946.
- [6] J.-S.Hong and M.J.Lancaster, "Coupling of Microstrip Square Open-Loop Resonators for Cross-Coupled Planar Microwave Filters," *IEEE Transaction on Microwave Theory and Technique*, vol.44, pp. 2099-2108, Dec. 1996.
- [7] J.-S.Hong and M.J.Lancaster, "Design of Highly Selective Microstrip Bandpass Filters with a Single Pair of Attenuation Poles at Finite Frequencies," *IEEE Transaction on Microwave Theory and Technique*, vol.48, pp. 1098-1107, July. 2000.
- [8] C.-S.Ahn, J.Lee, and Y.-S.Kim, "Design Flexibility of an Open-Loop Resonator Filter Using Similarity Transformation of Coupling Matrix," *IEEE Microwave and Wireless Components Letters*, Vol.15, No.4, pp. 262-264, April 2005.
- [9] C.Balanis, *Antenna Theory*. Canada: John Wiley & Sons, Inc, 1997.
- [10] D.M.Pozar, *Microwave Engineering*, 2<sup>nd</sup> ed. New York:Wiley, 1998.